

Article

## ***N*-Vinylcarbazole: As an Additive for Thermal Polymerization at Room Temperature with *in situ* Formation of Ag(0) Nanoparticules**

Mohamad-Ali Tehfe \*, Saïd Elkoun and Mathieu Robert

Carrefour of Innovative Technology and Ecodesign (CITE), Faculty of Engineering, University of Sherbrooke, 2500 boul. de l'Université, Sherbrooke, QC J1K 2R1, Canada;

E-Mails: Said.Elkoun@USherbrooke.ca (S.E.); Mathieu.Robert2@USherbrooke.ca (M.R.)

\* Author to whom correspondence should be addressed;

E-Mail: Mohamad.Ali.Tehfe@USherbrooke.ca; Tel.: +1-514-431-7436.

Academic Editor: Philippe Lambin

Received: 3 July 2015 / Accepted: 28 July 2015 / Published: 5 August 2015

---

**Abstract:** *N*-vinylcarbazole (NVK) is proposed as an additive for acrylates thermal free radical polymerization (FRP) and epoxy thermal ring opening polymerization (ROP) at room temperature. The new initiating systems are based on a silane/silver salt/*N*-vinylcarbazole interaction, which ensures good to excellent polymerization. Moreover, the polymerization is much more efficient under air than under argon. The effects of the *N*-vinylcarbazole, silane, silver salt and monomer structures are investigated. Interestingly, silver nanoparticles Ag(0) are formed *in situ*. The as-synthesized nanocomposite materials contained spherical nanoparticles homogeneously dispersed in the polymer matrices. Polymers and nanoparticles were characterized by Differential Scanning Calorimetry (DSC), Transmission Electron Microscopy (TEM), Energy-Dispersive X-ray Spectrometry (EDS), Fourier Transform Infrared Spectroscopy (FTIR), and UV-vis spectroscopy. A coherent picture of the involved chemical mechanisms is presented.

**Keywords:** *N*-vinylcarbazole; silane; silver salt; thermal free radical polymerization (FRP); thermal ring opening polymerization (ROP); silver nanoparticules

---

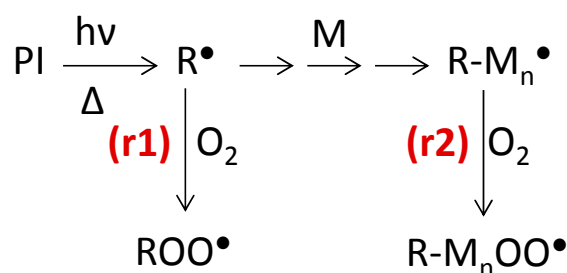
## 1. Introduction

Nanocomposite materials containing noble metal and dispersed nanoparticles in a polymer matrix may exhibit peculiar physical and chemical properties that are of high scientific and technological importance [1]. These new composites are used for optical [2], electrical [3] and medical [4] applications as well as data storage [5]. In particular, silver nanoparticles are very important for their excellent electrical conductivity [6], anti-microbial effect [7] and optical properties [8]. In recent years, a whole bunch of synthetic methods for the preparation of metal nanoparticules have been developed: chemical, photochemical and thermal.

Metal-polymer nanocomposites are usually obtained via multistep methods. Dry silver nanoparticules (NPs) produced beforehand can be dispersed into a polymerizable formulation to obtain self-assembly functionalized structures. However, besides the specific hazards related to handling dry NPs, their size dispersity over a large scale is difficult to control, thus limiting the interest of this “*ex situ*” method [9,10].

The “*in situ*” approach that involves the generation of metal nanoparticules directly in a polymerizable medium through reduction of cationic precursors offers the advantages of better dispersion ability and facile chemical or photochemical reduction [11,12].

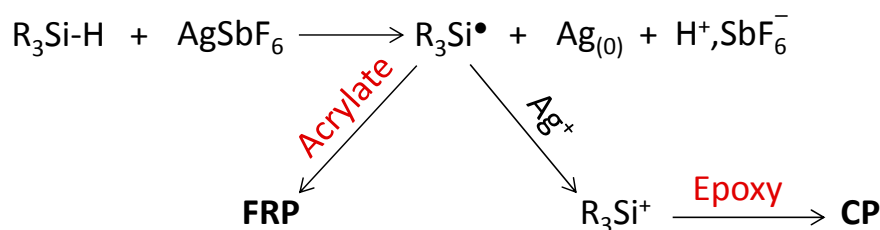
Thermally and photochemically induced free radical polymerizations (FRP) have been the subject of numerous studies [13–18]. In thermal FRPs, redox initiated processes are very attractive due e.g., to the absence of solvents and the use of quite low reaction temperatures. However, such FRPs suffer from a strong drawback concerned with the well-known oxygen inhibition [13–20]. Indeed, both the initiating (Scheme 1(r1)) and propagating (Scheme 1(r2)) radicals are scavenged by O<sub>2</sub> and converted into stable peroxy radicals, which cannot participate in any further polymerization initiation reactions and lead to a decrease of both polymerization rates and final conversions (Scheme 1) [21–24].



**Scheme 1.** Different polymerization reactions under oxygen (r1: initiating step and r2: propagation step).

In cationic polymerization (CP), such an inhibition does not exist and, interestingly, the use of less toxic monomers than the acrylates can be highly worthwhile. Redox systems being able to initiate a cationic polymerization have been already proposed [25–28]. Very recently, new bi-component combinations based on onium salt (diaryliodonium or triarylsulfonium salt) and organosilane (R<sub>3</sub>SiH) as the reducing agent were elegantly proposed: the redox reaction is catalyzed by noble metal complexes (platinum, palladium, rhodium) and leads to a silylium cation, which directly attacks the epoxide or/and reacts with water to form a Bronstedt acid [29].

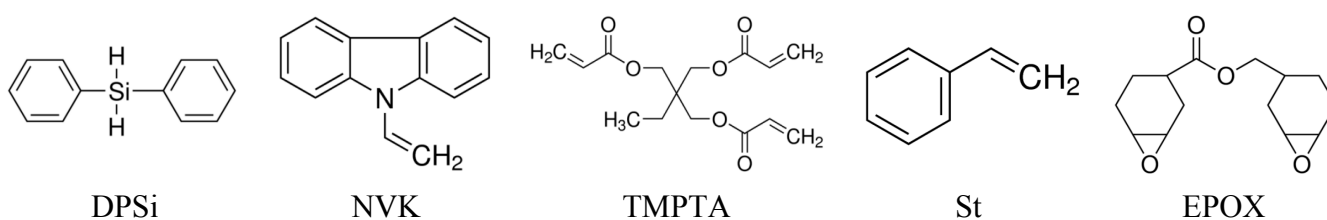
The thermal FRP and/or CP at room temperature and under air remain an exciting research topic. This approach consists of producing a radical  $R^\bullet$  (from an organosilane), to initiate FRP, that can be easily oxidized by a silver salt (e.g.,  $\text{AgSbF}_6$ ) leading to  $R^+$ , which corresponds to the ROP initiating structure (Scheme 2) [30–32].



**Scheme 2.** Schematic representation of the polymerization mechanisms.

However, the nature of the primary radicals produced from the organosilane is crucial for getting a high polymerization efficiency, as they should be characterized by excellent oxidation properties; moreover, the resulting radicals and cations must be efficient structures for the FRP and CP reactions, respectively [33–37]. Even if a lot of systems have been developed in the last years [33–42], the search for novel additives being able to improve the radical and/or cationic polymerization processes still appears as a challenge.

In the present paper, *N*-vinylcarbazole (NVK) is used as an additive for thermal free and/or cationic polymerization of an acrylate and an epoxide at room temperature and under air (TMPTA, St and EPOX—see below, Scheme 3). This proposal is the result of three approaches connected with (i) the fascinating and versatile use and potential of organosilanes in radical and cationic photopolymerization under air recently outlined [43–45]; (ii) the general interest for the *in situ* incorporation of metallic particles into a polymer film (*i.e.*, the insertion of  $\text{Ag}_{(0)}$  into a matrix is highly worthwhile for the design of biocide or bactericide incorporating polymers); and (iii) the formation of an excellent film-forming properties and the high glass-transition-temperature ( $220^\circ\text{C}$ ) due to the formation of polyvinylcarbazole (PVK) in the film of polymer [46,47].



**Scheme 3.** Investigated compounds for polymerization processes.

## 2. Experimental Section

### 2.1. Compounds

The compounds with the highest purity available used are presented in Scheme 3. Diphenylsilane (DPSi), *N*-Vinylcarbazole (NVK), Silver hexafluoroantimonate ( $\text{AgSbF}_6$ ), Trimethylol-propane triacrylate

(TMPTA), Styrene (St) and (3,4-epoxycyclohexane) methyl 3,4-epoxycyclohexylcarboxylate (EPOX) were all purchased from Sigma-Aldrich and used as received.

### 2.2. Radical and Cationic Polymerization

Silver salt (1% w/w) was dissolved in the selected monomer (TMPTA, St or EPOX) and diphenylsilane (DPSi) was introduced into the formulation by a syringe at room temperature. The polymerization of these monomers (TMPTA, St and EPOX) was carried out in pill-box for a sample of 1 g. The progress of the exothermic polymerization is followed by monitoring the sample temperature using a thermocouple connected to a DaqPro-5300 (resolution 0.1 °C, Spectris Canada, Inc; Dba Omega Environmental, Laval, Canada). A magnetic stirrer in contact with the pill-box was used to ensure a good homogeneity. The addition of the DPSi into the formulation corresponds to time  $t = 0$  s.

Since most radical or cationic polymerizations rapidly take place with the release of a large amount of heat (exothermic reaction), it has been shown [29,48] that the increase of the temperature is directly proportional to the monomer conversion. However, as the set-up used here is not adiabatic, the relationship between the conversion and the temperature is only valid for the first steps of the polymerization process.

### 2.3. Interpenetrated Polymer Network Synthesis

For the polymerization of TMPTA/EPOX (50%/50% w/w) blends, silver salt (1% w/w) was dissolved into the mixture of monomers and DPSi was introduced into the formulation by a syringe at RT. The polymerization of TMPTA/EPOX was carried out in pill-box for a sample of 1 g. The progress of the exothermic polymerization is followed by monitoring the sample temperature using a thermocouple connected to a DaqPro-5300 (resolution 0.1 °C). A magnetic stirrer in contact with the pill-box was used to ensure a good homogeneity. The addition of the DPSi into the formulation corresponds to time  $t = 0$  s.

### 2.4. Characterization

UV measurements were carried out with a Spectra max plus 384 spectrometer (VWR International; Mont Royal, QC, Canada), whereas Fourier-transform infrared spectra (FTIR) were performed on an ABB Bomen Spectrometer (ABB Bomen, Quebec, QC, Canada).

Elemental analysis was obtained by energy-dispersive X-ray spectrometry (EDS) using an EDS spectrometer (Oxford instruments Austin, Inc., Austin, TX, USA).

Differential Scanning Calorimetry (DSC) analysis was performed on a DSC-Q2000 instrument (TA instruments Inc., Mississauga, ON, Canada) under a nitrogen atmosphere at a heating or cooling rate of 20 °C/min. The films were scanned in the range of 25 °C to 300 °C.

Transmission electron microscopy (TEM) analyses of composite materials were carried out at an accelerated voltage of 80 kV using a Hitachi H-7500 TEM (Hitachi High Technologies Canada, Inc., Toronto, ON, Canada).

### 3. Results and Discussion

#### 3.1. Free Radical Polymerization (FRP)

The polymerization of TMPTA smoothly proceeds at room temperature using DPSi/AgSbF<sub>6</sub> (2%/1% w/w) (Figure 1A); the stirring is stopped within 3 min due to the complete polymerization of the formulation. The polymerization does not occur using DPSi or AgSbF<sub>6</sub> independently thereby demonstrating that this combination is necessary to initiate the process. Almost no inhibition is noted as a short period is already requested for the solubilization of the silane into the formulation. A complete polymerization is obtained after about 300 s. It can be noted that the polymerization is dramatically faster under air than under argon (tack free time ~3 min vs. 6 min, respectively, Figure 1A). This result shows that (i) no strong oxygen inhibition obviously occurs; and (ii) oxygen should positively participate in the initiation process (see below). Remarkably, a high Si-H consumption is observed during the polymerization (Figure 1B) confirming the hydrogen abstraction process (Schemes 2 and 3) (see below): This demonstrates that the Si-H conversion is directly related to the overall efficiency of the system. The formation of polyacrylate (PTMPTA) is well evidenced by IR spectra by the observation of the disappearance of the characteristic band of the acrylate double bonds at 1620 cm<sup>-1</sup> (Figure 1C) [10,49].

Interestingly, the addition of NVK strongly improves the polymerization profiles, *i.e.*, both the polymerization rate and the conversion are higher in the presence of NVK (the increase of the temperature is directly proportional to the monomer conversion [29,48]) (Figure 2). A decrease of the tack free time is also noted (*i.e.*, ~1 min vs. 3 min with and without NVK, respectively). Remarkably, no polymerization is observed when using NVK/AgSbF<sub>6</sub> system in the same conditions (*i.e.*, room temperature and under air). Consequently, the different three-component system (Silane/NVK/Silver salt) can be considered as excellent initiating system for thermal free radical polymerization under air and at RT (Figure 2).

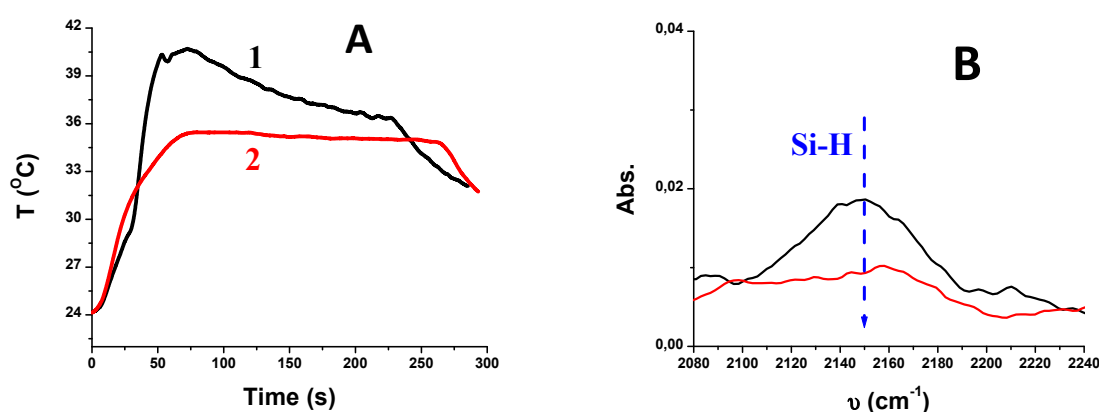
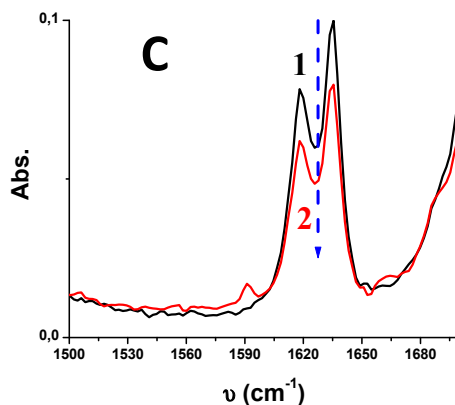
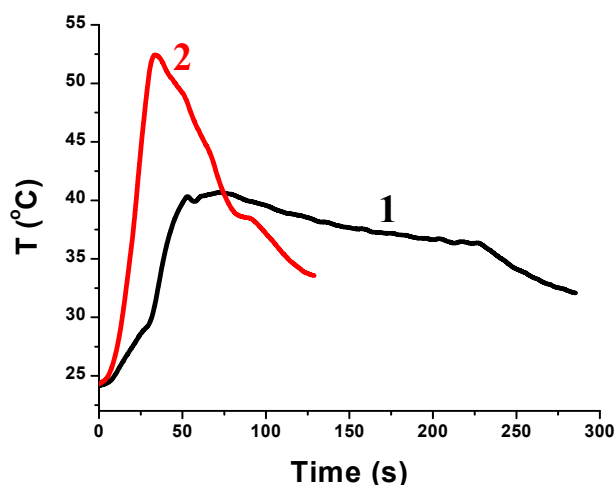


Figure 1. Cont.



**Figure 1.** (A) Role of the atmosphere in the free radical polymerization of TMPTA in the presence of DPSi/AgSbF<sub>6</sub> (2%/1% w/w): (1) under air and (2) under argon; (B) IR band of the decreasing of the DPSi recorded during the polymerization; and (C) real-time FT-IR spectra in the 1600–1670 cm<sup>-1</sup> wavenumber range of sample containing 1% (wt) of AgSbF<sub>6</sub> and 2% (wt) of DPSi in TMPTA under air (1- before and 2- after polymerization).



**Figure 2.** Comparison of the polymerization initiating ability under air and at RT of sample containing 1% (wt) of AgSbF<sub>6</sub> and 2% (wt) of DPSi in TMPTA: (1) without NVK and (2) with 2% (wt) of NVK.

However, the great interest of the proposed approach lies on the fact that the initiating system is efficient using simple glass vials and unpurified TMPTA, even in the presence of water or oxygen, which can act as polymerization inhibitors with other synthetic approaches [50]. This can open new opportunities for mass production and applications of PTMPTA.

Interestingly, when using a styrene monomer (St) instead TMPTA in the same experimental conditions, FRP occurs but the process is less efficient (e.g., inhibition time is high and tack free time ~4 h using St vs. no inhibition time and 1 min using TMPTA) (Figure 3A). This can be related to the low viscosity of this monomer (0.762 cp) compared to that of TMPTA (70–100 cp), which increases the oxygen inhibition [33,51]. The formation of polystyrene (PSt) is well evidenced by IR spectra of the obtained polymer (Figure 3B), which are fully consistent with the spectra that show the disappearance of the characteristic band of the acrylate double bonds at 1630 cm<sup>-1</sup>. Remarkably, the

consumption of the silanes Si-H is almost complete ( $\sim 100\%$ ) (Figure 3C). This is also found in agreement with the proposed mechanism (Schemes 1 and 2).

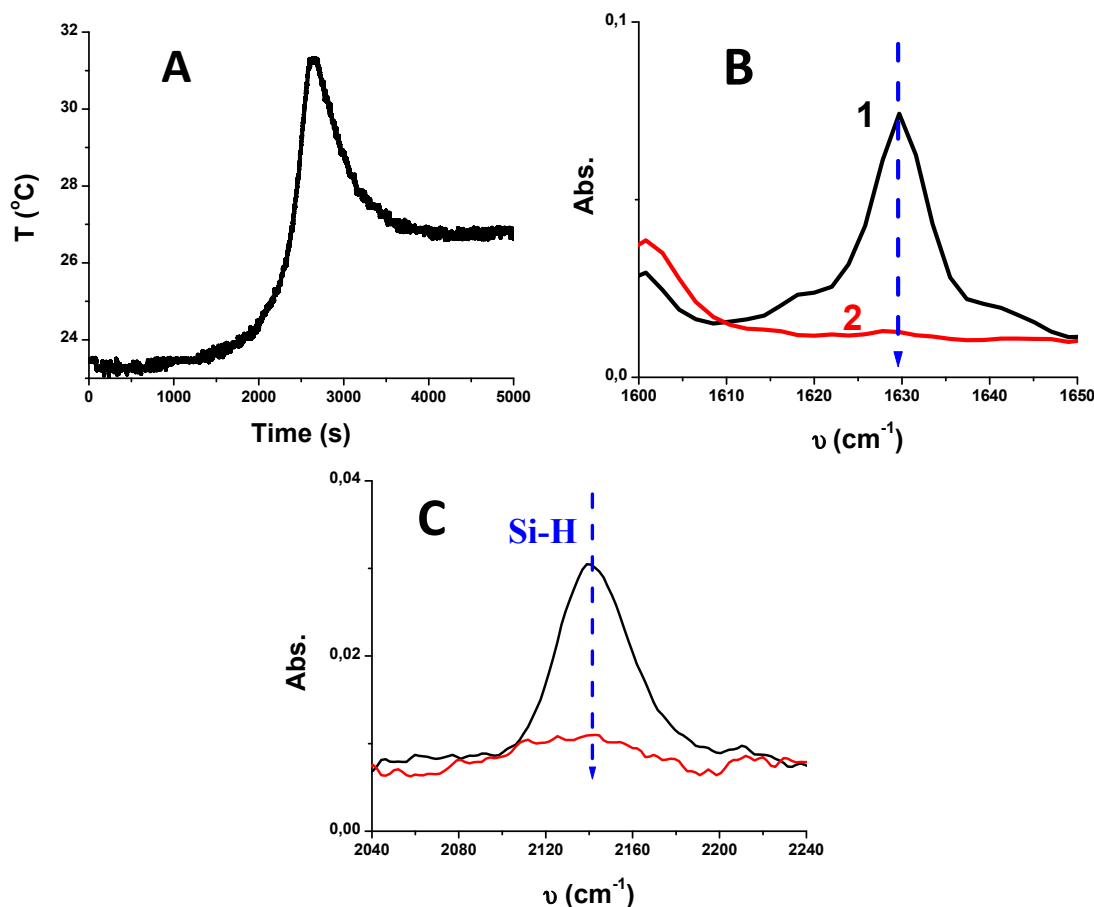


**Figure 3.** (A) Role of the monomer in the thermal free radical polymerization of Styrene (St) under air in the presence of DPSi/NVK/AgSbF<sub>6</sub> (2%/2%/1% w/w); (B) real-time FT-IR spectra in the 1600–1650 cm<sup>-1</sup> wavenumber range of sample containing 1% (wt) of AgSbF<sub>6</sub>, 2% (wt) of NVK and 2% (wt) of DPSi in Styrene under air (1) before and (2) after polymerization; and (C) IR band of the decreasing of the DPSi recorded during the polymerization.

### 3.2. Cationic Polymerization (CP)

Interestingly, the proposed new system (DPSi/NVK/AgSbF<sub>6</sub>) is quite versatile since they are also able to initiate the polymerization of epoxy monomers, such as (3,4-Epoxy cyclohexane) methyl 3,4-epoxycyclohexylcarboxylate (EPOX), which indicates that the formation of the cationic species is also efficient in this case (Figure 4A). A quite good polymerization is always obtained at RT and under air leading to tack free surface coatings (gel time  $\sim 5$  min and tack free time  $\sim 1$  h). It is evident the important decrease of the typical epoxy band at 770–830 cm<sup>-1</sup> and the high increase of the band at 1080 cm<sup>-1</sup> due to ether group formed during the ring-opening polymerization (Figure 4B) [30–37]. Almost no inhibition is noted, as a short period is already requested for the solubilization of the silane into the formulation.

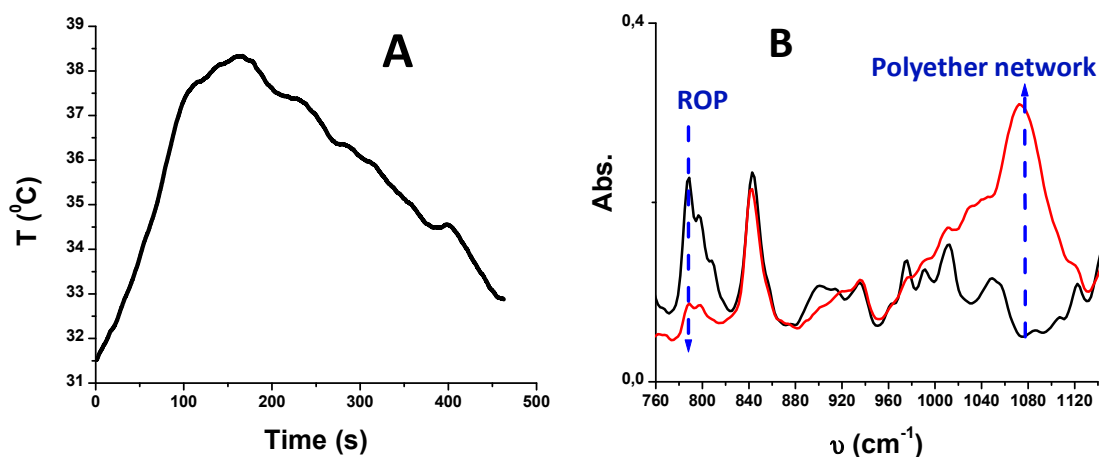


**Figure 4.** (A) Role of the monomer in the thermal free radical polymerization of EPOX under air in the presence of DPSi/NVK/AgSbF<sub>6</sub> (2%/2%/1% w/w). (B) IR spectra recorded during the thermal cationic polymerization in the range between 760–1140 cm<sup>-1</sup> of sample containing 1% (wt) of AgSbF<sub>6</sub>, 2% (wt) of DPSi and 2% (wt) of NVK in EPOX (1) before and (2) after polymerization.

### 3.3. DPSi/NVK/AgSbF<sub>6</sub> for the Synthesis of Interpenetrated Polymer Networks (IPNs)

The new system (DPSi/NVK/AgSbF<sub>6</sub>) that simultaneously and efficiently generates initiating radicals and cations (see below, r4) can allow an easy synthesis of interpenetrated polymer network from TMPTA/EPOX blend (50%/50%) by thermal polymerization at RT and under air (Figure 5A). They ensure good to excellent polymerizations are always obtained leading to tack free surface coatings after only 3 min. A concomitant increase of the band at 1080 cm<sup>-1</sup> and decrease of the band at 1620 cm<sup>-1</sup> is also observed due to the formation of the polyether network and polyacrylate, respectively (Figure 5B) [30–32]. A high Si-H consumption is also found in agreement with the proposed mechanisms (Schemes 1 and 2) (Figure 5C). Remarkably, a decrease of the concentration of DPSi reduces the efficiency of polymerization: a decrease of the temperature and an increase of the tack free time is also noted (*i.e.*, 3 and 5 min for 2 and 1% w/w of DPSi, respectively) (Figure 5D). This demonstrates that the silane concentration is directly related to the overall efficiency of the system.

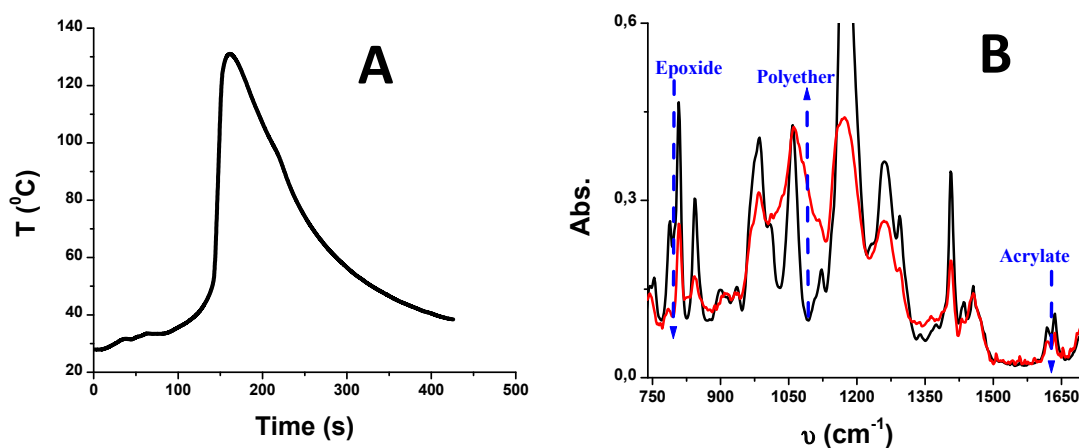


**Figure 5.** Cont.

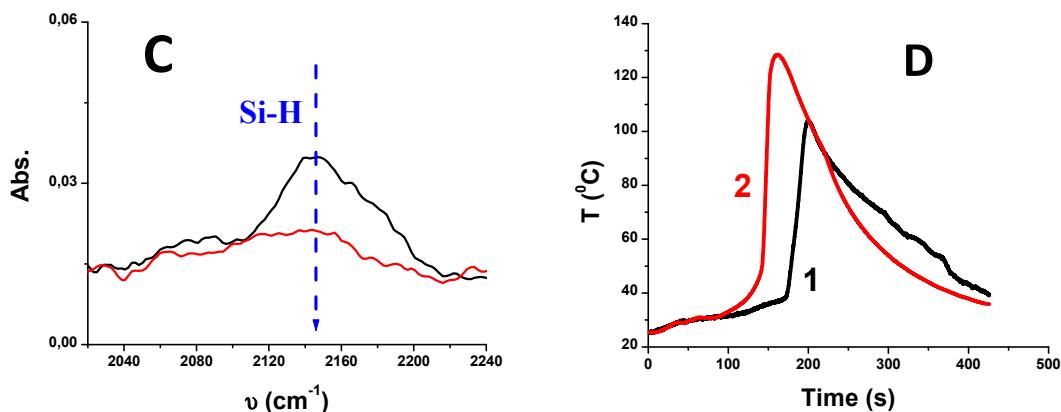


**Figure 5.** (A) Role of the organosilane in the thermal interpenetrated polymer networks (IPNs) of TMPTA/EPOX blend (50%/50%) under air in the presence of DPSi/NVK/AgSbF<sub>6</sub> (2%/2%/1% w/w). (B) IR spectra recorded during the thermal IPN polymerization of the TMPTA/EPOX blend (50%/50%) of sample containing 1% (wt) of AgSbF<sub>6</sub>, 2% (wt) of DPSi and 2% (wt) of NVK (1) before and (2) after polymerization. (C) IR band of the decreasing of the DPSi recorded during the polymerization. (D) Role of the concentration of organosilane in the thermal interpenetrated polymer networks (IPNs) of TMPTA/EPOX blend (50%/50%) under air in the presence of NVK/AgSbF<sub>6</sub> (2%/1% w/w): (1) with 1% (wt) DPSi and (2) 2% (wt) DPSi.

### 3.4. In-situ Incorporation of Silver Nanoparticles (Ag(0)NPs)

The *in-situ* formation of silver nanoparticles (Ag(0)NPs) during the polymerization process is demonstrated by UV-visible spectroscopy (Figure 6). The addition of DPSi to AgSbF<sub>6</sub> in TMPTA, St or EPOX monomers leads to the formation of Ag(0) nanoparticles clearly evidenced by UV-visible spectroscopy (*i.e.*, surface plasmon resonance (SPR) band typical of silver nanoparticles observed at about 405 nm (Figure 6)). Unprotected Ag(0) nanoparticles characterized by the size domain < 15 nm display a SPR band at a similar wavelength [52,53].

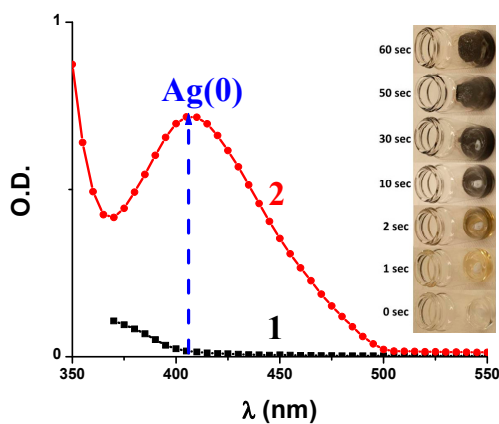
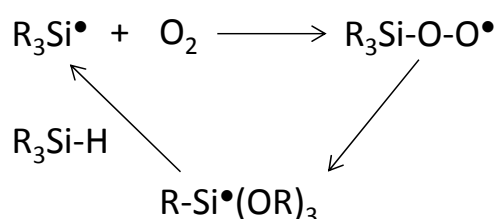


**Figure 6.** UV-visible absorption spectra of a polymerized TMPTA film using AgSbF<sub>6</sub> (1% w/w) and NVK (2% w/w) in the absence (1) and in the presence (2) of DPSi (2% w/w); Insert: Evolution of Ag(0)NPs colors during the synthesis in TMPTA at RT and under air.

### 3.5. Reaction Mechanisms

The formation of a silyl radicals ( $R_3Si^\bullet$ ) and/or silylium cations ( $R_3Si^+$ ) through the interaction of the silane with silver salt is assumed (Scheme 2) by analogy with the reported behavior of  $R_3SiH/AgOCl_4$  in organic chemistry [54–57]. These reactions might proceed by an attack of the electrophile on a Si-H bond [54–57]. On the other side, the formation of silylium cations when using chlorosilanes ( $R_3SiCl$ ) instead of  $R_3SiH$  with silver salts (r'1) was well characterized [58]. The good polymerization ability of the  $R_3SiH/AgSbF_6$  and  $R_3SiH/AgSbF_6/NVK$  systems appears here as in full agreement with the formation of  $R_3Si^\bullet$ ,  $NVK^\bullet$ ,  $R_3Si^+$ ,  $NVK^+$  and  $H^+$ , which are largely known [16,17,43–45,59–62] as efficient initiating species for both thermal and photochemical radical and/or cationic polymerization of TMPTA and EPOX.

Scheme 2, however, does not account for the favorable oxygen effect. The mechanism (Scheme 4) involves the oxidation of the silyl radical into a peroxy, a rearrangement of the peroxy (as already observed elsewhere) [63] and the further re-generation of a silyl radical together with the formation of  $R-SiH(O-R)_2$ . Such a process was already reported in [63,64].

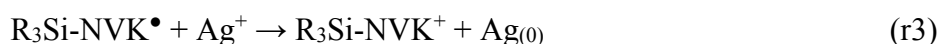
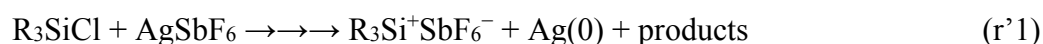


**Scheme 4.** Kinetics of rearrangement of the peroxy radicals into silyl radicals.

Upon addition of NVK,  $R_3Si^\bullet$  react with the NVK double bond leading to  $R_3Si-NVK^\bullet$  (r'2), as known in other systems [59–62]. As previously discussed [59–62],  $R_3Si-NVK^\bullet$  radicals are easily oxidized by  $Ag^+$  leading to the formation of  $R_3Si-NVK^+$  (r3) [65,66].  $R_3Si-NVK^\bullet$  is characterized by a very low ionization potential [60]; this is fully consistent with the associated fast oxidation process.

The  $R_3Si-NVK^\bullet$  and  $R_3Si-NVK^+$  being a highly efficient initiating structure for the FRP and ROP of an acrylate and an epoxy [59,65–67], it is not surprising that an efficient polymerization is found in the presence of NVK.

In these reactions, radicals and cations are probably generated to initiate the free radical polymerization (FRP), ring opening polymerization (ROP) and interpenetrated polymer network (IPN) of the acrylate, epoxy and acrylate/epoxy blend monomers (r4), respectively, with *in-situ* formation of silver nanoparticles ( $Ag(0)NPs$ ) during the polymerization process (see above). Other elegant initiating systems based on other radical oxidation processes by  $Ag^+$  were proposed in ref [68–75].



### 3.6. Characterization of Ag(0) Nanoparticles (NPs) and Polymer Films

Functionalized Ag(0)NPs were characterized by TEM and EDX. The bright field transmission electron microscopy images (TEM) of films cured using AgSbF<sub>6</sub>/NVK/DPSi (1%/2%/2% w/w) system dissolved in different monomers (TMPTA, St or EPOX) are reported in Figure 7. The TEM micrograph (Figure 7) of Ag(0)NPs obtained after thermal polymerization at RT shows that the Ag(0)NPs remain well-dispersed in the polymer matrix and are well dispersed with no significant agglomeration. A spherical geometry was noticed of the particles whose diameters are in the 5 to 25 nanometer range. The TEM images suggest the possibility of a homogeneous polymeric coating on the nanoparticle surface. These morphological results are in agreement with ref [10,62,72,76].

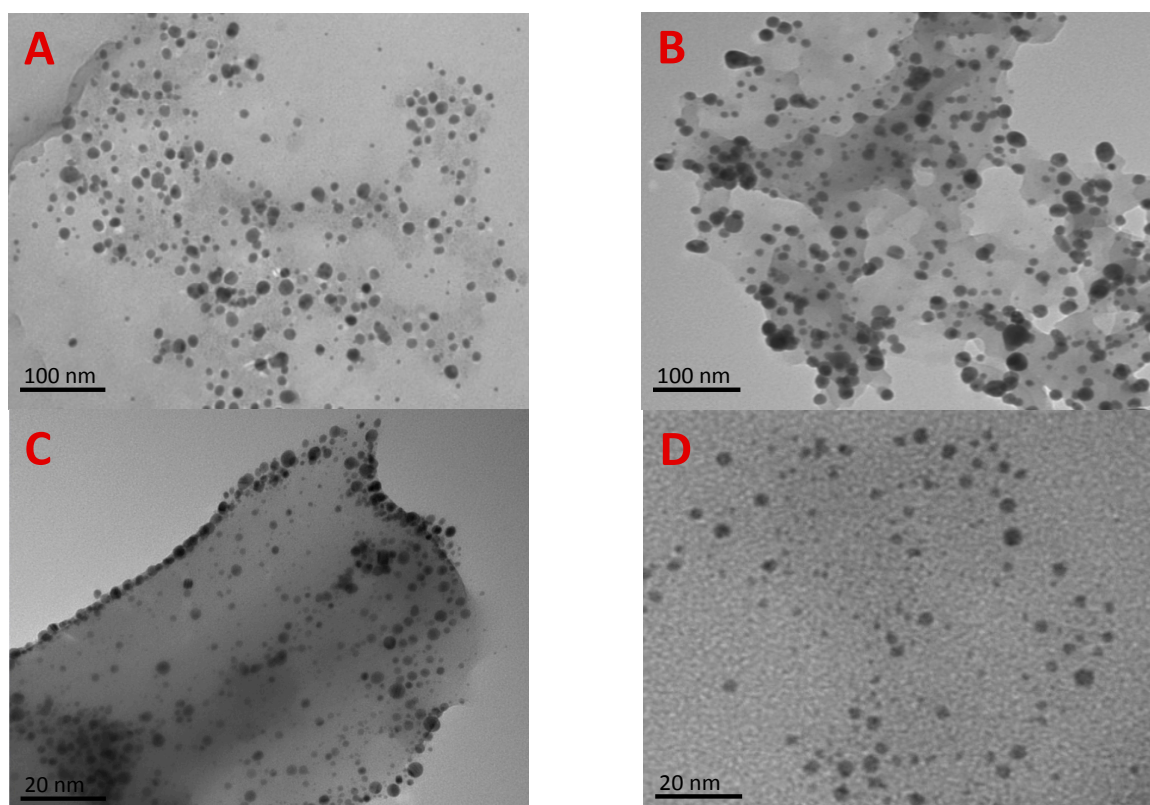


**Figure 7.** TEM analysis of silver nanoparticles obtained after thermal polymerization using AgSbF<sub>6</sub>/NVK/DPSi (1%/2%/2% w/w) system in (A) TMPTA, (B) St, (C) EPOX and (D) IPN (TMPTA/EPOX).

The formation of Ag(0)NPs created *in situ* in this hybrid polymer matrix during thermal radical and/or cationic polymerization at room temperature were monitored using energy dispersive X-ray (EDS) spectroscopy analysis, as shown in Figure 8. Indeed, in the resulting EDS pattern, C, O, F, Si, Au, Ag and Sb peaks are clearly shown, demonstrating that silver/polymer composites were successfully prepared by this one-step process. Remarkably, the presence of Au(0) particles is due to the phenomenon of metallization of the polymer matrix before making the measurement.

Thermal behavior of the cured films was evaluated by DSC measurements. The DSC curves are reported in Figure 9. Remarkably, a clear increase of the glass-transition-temperature (T<sub>g</sub>) values after addition of *N*-vinylcarbazole (NVK) in the formulations was noted (*i.e.*, 226 °C for curve 2 vs. 212.5 °C for

curve 1, Figure 9). The reason for such an increase is due to the formation of polyvinylcarbazole (PVK) in the film of polymer, which leads to (1) a decrease of the free volume; and (2) the impediment of the mobility crosslinked epoxide and/or an acrylate polymer network.

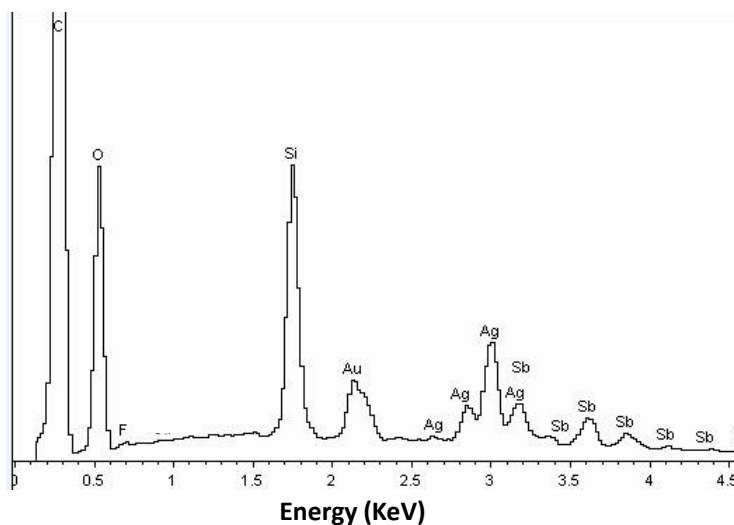


**Figure 8.** Energy-Dispersive X-ray Spectrometry (EDS) analysis recorded from Ag(0) nanoparticles in EPOX.

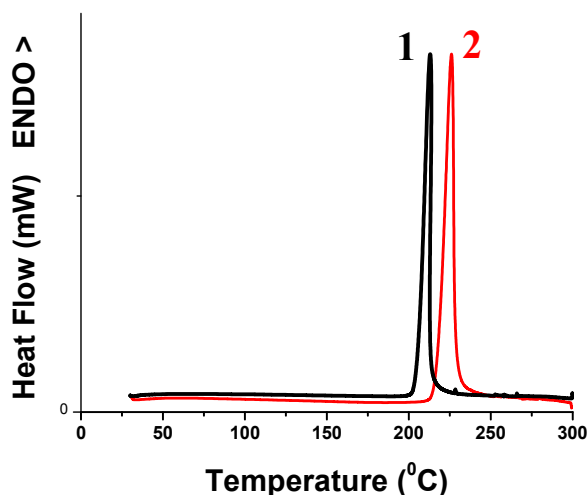


**Figure 9.** DSC thermograms for the cured samples containing (1) DPSi/AgSbF<sub>6</sub> (2%/1% w/w) and (2) DPSi/NVK/AgSbF<sub>6</sub> (2%/2%/1% w/w) in TMPTA.

#### 4. Conclusions

In the present study, *in situ* synthesis of silver-acrylate, silver-epoxy and silver-IPN nanocomposites was achieved by thermal polymerization through a simultaneous radical and/or cationic polymerization processes using a silane/silver salt couple at room temperature and under air. Remarkably, and unlike published works so far, heating is not required to activate the reaction. The new redox systems were proposed to initiate in two-component systems (DPSi/silver salt) the ring-opening polymerization (ROP) of (3,4-Epoxycyclohexane) methyl 3,4-epoxycyclohexylcarboxylate (EPOX) and the free radical polymerization (FRP) of trimethylolpropane triacrylate (TMPTA) and styrene (St).

Interestingly, the addition of *N*-Vinylcarbazole (NVK) to the silane/silver salt systems leads to a drastic increase of polymerization reactivity and efficiency, respectively. This three-component system generates free radicals ( $R_3Si^\bullet$  and  $NVK^\bullet$ ) or ions ( $R_3Si^+$ ,  $NVK^+$  and  $H^+$ ). Remarkably, fast ROP and FRP are observed. Interestingly, these initiators can also be used for the synthesis of interpenetrated polymer networks (IPN), e.g., for the polymerization of TMPTA/EPOX blends. Highly crosslinked network were achieved and the nanocomposite obtained, contains near spherical geometry for most of the nanoparticles, homogeneously dispersed in the polymer network without significant agglomeration as a result of a surrounding effect of polymer chains formed by the rapid cationic and/or radical chain growth. Interestingly, an increase on  $T_g$  values was observed after addition of *N*-vinylcarbazole (NVK) in the formulations. This was ascribed to a decrease of free volume of the polymer network because the formation of PVK in the film of polymer leads in the impediment of the mobility crosslinked epoxide and/or an acrylate polymer network. The mechanical and optical properties of the obtained new organic polymer/silver nanoparticles will be investigated in near future.

### Author Contributions

Hereby, the three authors of the paper testify that we have contributed substantially to the study design, data analysis and manuscript writing and revision. Study conception and design were done by M.-A.T., S.E. and M.R. Experimental part was carried out by M.-A.T. Data analysis and interpretation were performed by M.-A.T., S.E. and M.R. Drafting of manuscript and revision were carried out by M.-A.T., S.E. and M.R.

### Conflicts of Interest

The authors declare no conflicts of interest.

### References

1. Carotenuto, G.; Martorana, B.; Perlo, P.B.; Nicolais, L. A universal method for the synthesis of metal and metal sulfide clusters embedded in polymer matrices. *J. Mater. Chem.* **2003**, *13*, 2927–2930.
2. Biswas, A.; Aktas, O.C.; Schurmann, U.; Saeed, U.; Zaporojtchenko, V.; Faupel, F. Controlled syntheses of Ag-polytetrafluoroethylene nanocomposite thin films by co-sputtering from two magnetron sources. *Appl. Phys. Lett.* **2004**, *84*, 2655–2657.
3. Sih, B.C.; Wolf, M.O. Metal nanoparticle—Conjugated polymer nanocomposites. *Chem. Commun.* **2005**, *27*, 3375–3384.
4. Fan, F.R.F.; Bard, A.J. Chemical, electrochemical, gravimetric, and microscopic studies on antimicrobial silver films. *J. Phys. Chem. B* **2002**, *106*, 279–287.
5. Ouyang, J.Y.; Chu, C.W.; Szmanda, C.R.; Ma, L.P.; Yang, Y. Programmable polymer thin film and non-volatile memory device. *Nat. Mater.* **2004**, *3*, 918–922.
6. Chang, L.T.; Yen, C.C. Studies on the preparation and properties of conductive polymers. VIII. Use of heat treatment to prepare metallized films from silver chelate of PVA and PAN. *J. Appl. Polym. Sci.* **1995**, *55*, 371–374.

7. Shanmugam, S.; Viswanathan, B.; Varadarajan, T.K. A novel single step chemical route for noble metal nanoparticles embedded. *Mater. Chem. Phys.* **2006**, *95*, 51–55.
8. Lin, W.C.; Yang, M.C. Novel Silver/Poly(vinyl alcohol) Nanocomposites for Surface-Enhanced Raman Scattering-Active Substrates. *Macromol. Rapid Commun.* **2005**, *26*, 1942–1947.
9. Balan, L.; Burget, D. Synthesis of metal/polymer nanocomposite by UV-radiation curing. *Eur. Polym. J.* **2006**, *42*, 3180–3189.
10. Balan, L.; Schneider, R.; Loughnot, D.J. A new and convenient route to polyacrylate/silver nanocomposites by light-induced cross-linking polymerization. *Prog. Org. Coat.* **2008**, *62*, 351–357.
11. Selvan, S.T.; Spatz, J.P.; Klok, H.A.; Möller, M. Gold–Polypyrrole Core–Shell Particles in Diblock Copolymer Micelles. *Adv. Mater.* **1998**, *10*, 132–134.
12. Corbierre, M.K.; Cameron, N.S.; Sutton, M.; Mochrie, S.G.; Lurio, L.B.; Rühm, A.; Lennox, R.B. Polymer-Stabilized Gold Nanoparticles and Their Incorporation into Polymer Matrices. *J. Am. Chem. Soc.* **2001**, *123*, 10411–10412.
13. Matyjaszewski, K.; Gnanou, Y.; Leibler, L. *Macromolecular Engineering: From Precise Macromolecular Synthesis to Macroscopic Materials Properties and Applications*; Wiley-VCH: Weinheim, Germany, 2007.
14. Pappas, S.P. *UV Curing: Science and Technology*; Technology Marketing Corp: Aachen, Germany, 1985.
15. Dietliker, K. *A Compilation of Photoinitiators Commercially Available for UV Today*; Sita Technology Ltd.: Edinburgh, UK; London, UK, 2002.
16. Crivello, J.V. *Photoinitiators for Free Radical, Cationic and Anionic Photopolymerization*, 2nd ed.; Bradley, G., Ed.; Wiley & Sons: New York, NY, USA, 1998.
17. Crivello, J.V. *Ring-Opening Polymerization*; Brunelle, D.J., Ed.; Hanser: Munich, Germany, 1993.
18. Sangermano, M.; Crivello, J.V. *Photoinitiated Polymerization*; Belfied, K.D., Crivello, J.V., Eds.; ACS Symposium Series 847: Washington, DC, USA, 2003.
19. Fouassier, J.P. *Photoinitiation Photopolymerization and Photocuring: Fundamental and Applications*; Hanser Publishers: New York, NY, USA, 1995.
20. *Radiation Curing in Polymer Science and Technology*; Fouassier, J.P., Rabek, J.F., Eds.; Elsevier Science Publishers Ltd.: London, UK, 1993.
21. El-Roz, M.; Lalevée, J.; Allonas, X.; Fouassier, J.P. Mechanistic Investigation of the Silane, Germane, and Stannane Behavior When Incorporated in Type I and Type II Photoinitiators of Polymerization in Aerated Media. *Macromolecules* **2009**, *42*, 8725–8732.
22. Hoyle, C.E.; Kim, K.-J. Photoinitiated polymerization of 1,6-hexanediol diacrylate-amine synergists. *J. Rad. Curing* **1985**, *12*, 9–15.
23. Decker, C.; Jenkins, A.D. Kinetic approach of oxygen inhibition in ultraviolet- and laser-induced polymerizations. *Macromolecules* **1985**, *18*, 1241–1244.
24. Gou, L.; Opheim, B.; Scranton, A.B. *Photochemistry and UV Curing: New Trends*; Fouassier, J.P., Ed.; Research Signpost: Trivandrum, India, 2006.
25. Crivello, J.V.; Lam, J.H.W. Redox cationic polymerization: The diaryliodonium salt/ascorbate redox couple. *J. Polym. Sci. Part A: Polym. Chem.* **1981**, *19*, 539–548.
26. Crivello, J.V.; Lee, J. Redox initiators for cationic polymerization: The diaryliodonium Salt/Sn(II) redox couple. *Makromol. Chem.* **1983**, *184*, 463–473.

27. Onen, A.; Yagci, Y. Redox-initiated cationic polymerization: The pyridinium salt/ascorbate redox couple. *Polymer* **1997**, *38*, 1423–1425.
28. Onen, A.; Denizligil, S.; Yagci, Y. Cationic polymerization using allyl sulfonium salt. 3. Allyl sulfonium salt/ascorbate redox couple. *Angew. Makromol. Chem.* **1997**, *245*, 149–154.
29. Crivello, J.V. Redox initiated cationic polymerization. *J. Polym. Sci. Part A: Polym. Chem.* **2009**, *47*, 1825–1835.
30. Souane, R.; Tehfe, M.-A.; Lalevée, J.; Gigmès, D.; Fouassier, J.-P. New Initiating Systems for Thermal Cationic Polymerization at Ambient Temperature with *in situ* Formation of Ag(0) Nanoparticles: A Silane/Silver Salt Combination. *Macromol. Chem. Phys.* **2010**, *211*, 1441–1445.
31. Tehfe, M.-A.; Jamois, R.; Cousin, P.; Elkoun, S.; Robert, M. *In situ* synthesis and characterization of silver/polymer nanocomposites by thermal cationic polymerization processes at room temperature: Initiating systems based on organosilanes and starch nanocrystals. *Langmuir* **2015**, *31*, 4305–4315.
32. Yagci, Y.; Sahin, O.; Ozturk, T.; Marchi, S.; Grassini, S.; Sangermano, M. Synthesis of silver/epoxy nanocomposites by visible light sensitization using highly conjugated thiophene derivatives. *React. Funct. Polym.* **2011**, *71*, 857–862.
33. Lalevée, J.; Tehfe, M.A.; Morlet-Savary, F.; Allonas, X.; Graff, B.; Fouassier, J.P. Oxygen mediated and wavelength tunable cationic photopolymerization reactions under air and low intensity: A new concept. *Prog. Org. Coat.* **2011**, *70*, 23–31.
34. Lalevée, J.; Blanchard, N.; Tehfe, M.A.; Morlet-Savary, F.; Fouassier, J.P. Green Bulb Light Source Induced Epoxy Cationic Polymerization under Air Using Tris(2,20-bipyridine)ruthenium(II) and Silyl Radicals. *Macromolecules* **2010**, *43*, 10191–10195.
35. Lalevée, J.; Blanchard, N.; Tehfe, M.A.; Peter, M.; Morlet-Savary, F.; Gigmès, D.; Fouassier, J.P. Efficient dual radical/cationic photoinitiator under visible light: A new concept. *Polym. Chem.* **2011**, *2*, 1986–1991.
36. Lalevée, J.; Blanchard, N.; Tehfe, M.A.; Peter, M.; Morlet-Savary, F.; Fouassier, J.P. A Novel Photopolymerization Initiating System Based on an Iridium Complex Photocatalyst. *Macromol. Rapid Commun.* **2011**, *32*, 917–920.
37. Lalevée, J.; Blanchard, N.; Tehfe, M.A.; Peter, M.; Morlet-Savary, F.; Fouassier, J.P. Household LED irradiation under air: Cationic polymerization using iridium or ruthenium complex photocatalysts. *Polym. Bull.* **2011**, *68*, 341–347.
38. Durmaz, Y.Y.; Moszner, N.; Yagci, Y. Visible Light Initiated Free Radical Promoted Cationic Polymerization Using Acylgermane Based Photoinitiator in the Presence of Onium Salts. *Macromolecules* **2008**, *41*, 6714.
39. Crivello, J.V. A new visible light sensitive photoinitiator system for the cationic polymerization of epoxides. *J. Polym. Sci. Part A: Polym. Chem.* **2009**, *47*, 866–875.
40. Crivello, J.V. Radical-Promoted Visible Light Photoinitiated Cationic Polymerization of Epoxides. *J. Macromol. Sci. Part A* **2009**, *46*, 474–483.
41. Tunc, D.; Yagci, Y. Thioxanthone-ethylcarbazole as a soluble visible light photoinitiator for free radical and free radical promoted cationic polymerizations. *Polym. Chem.* **2011**, *2*, 2557–2563.

42. Yilmaz, G.; Beyazit, S.; Yagci, Y. Visible light induced free radical promoted cationic polymerization using thioxanthone derivatives. *J. Polym. Sci. Part A: Polym. Chem.* **2011**, *49*, 1591–1596.
43. Lalevée, J.; Blanchard, N.; El-Roz, M.; Graff, B.; Allonas, X.; Fouassier, J.P. New Photoinitiators Based on the Silyl Radical Chemistry: Polymerization Ability, ESR Spin Trapping, and Laser Flash Photolysis Investigation. *Macromolecules* **2008**, *41*, 4180–4186.
44. Lalevée, J.; El-Roz, M.; Allonas, X.; Fouassier, J.P. Free-radical-promoted cationic photopolymerization under visible light in aerated media: New and highly efficient silane-containing initiating systems. *J. Polym. Sci. Part A: Polym. Chem.* **2008**, *46*, 2008–2014.
45. Tehfe, M.A.; Lalevée, J.; Allonas, X.; Fouassier, J.P. Long Wavelength Cationic Photopolymerization in Aerated Media: A Remarkable Titanocene/Tris(trimethylsilyl)silane/Onium Salt Photoinitiating System. *Macromolecules* **2009**, *42*, 8669–8674.
46. Uygun, M.; Kahveci, M.U.; Odaci, D.; Timur, S.; Yagci, Y. Antibacterial Acrylamide Hydrogels Containing Silver Nanoparticles by Simultaneous Photoinduced Free Radical Polymerization and Electron Transfer Processes. *Macromol. Chem. Phys.* **2009**, *210*, 1867–1875.
47. Dawson-Andoh, B.; Matuana, L. High density polyethylene-wood flour composite lumber: Efficacy of two proprietary biocides in the control of fungal colonization and discoloration. *Eur. J. Wood Wood Products* **2007**, *65*, 331–334.
48. Crivello, J.V. Redox initiated cationic polymerization: Reduction of diaryliodonium salts by 9-BBN. *J. Polym. Sci. Part A: Polym. Chem.* **2009**, *47*, 5639–5651.
49. Tehfe, M.-A.; Dumur, F.; Telitel, S.; Gignes, D.; Contal, E.; Bertin, D.; Morlet-Savary, F.; Graff, B.; Fouassier, J.-P.; Lalevée, J. Zinc-based metal complexes as new photocatalysts in polymerization initiating systems. *Eur. Polym. J.* **2013**, *49*, 1040–1049.
50. Kunioka, M.; Wang, Y.; Onozawa, S-Y. Polymerization of Poly( $\epsilon$ -caprolactone) Using Yttrium Triflate. *Polym. J.* **2003**, *35*, 422–429.
51. Lalevée, J.; Dirani, A.; El Roz, M.; Graff, B.; Allonas, X.; Fouassier, J.P. Silanes as New Highly Efficient Co-initiators for Radical Polymerization in Aerated Media. *Macromolecules* **2008**, *41*, 2003–2010.
52. Taleb, A.; Petit, C.; Pileni, M.P. Optical Properties of Self-Assembled 2D and 3D Superlattices of Silver Nanoparticles. *J. Phys. Chem. B* **1998**, *102*, 2214–2220.
53. He, S.; Yao, J.; Jiang, P.; Shi, D.; Zhang, H.; Xie, S.; Pang, S.; Gao, H. Formation of Silver Nanoparticles and Self-Assembled Two-Dimensional Ordered Superlattice. *Langmuir* **2001**, *17*, 1571–1575.
54. Eaborn, C. The reaction between trisubstituted silanes and silver perchlorate. Organosilicon Compounds. XIV. *J. Chem. Soc.* **1955**, *3*, 2517–2519.
55. Marciniak, B. Mechanism of competitive-consecutive reaction of trisubstituted silanes with silver perchlorate in benzene. *Z. Anorg. Allg. Chem.* **1982**, *495*, 232–240.
56. Ouellette, R.J.; Marks, D.L.; Miller, D.; Kesatie, D. Oxidation of silanes. III. Reaction of aryldimethylsilanes with mercuric acetate and thallium triacetate. *J. Org. Chem.* **1969**, *34*, 1769–1771.
57. Ouellette, R.J.; Marks, D.L. Oxidation of silanes II. The reaction of ozone with aryldimethylsilanes. *J. Organomet. Chem.* **1968**, *11*, 407–413.

58. Lambert, J.B.; Kania, L.; Zhang, S. Modern Approaches to Silylium Cations in Condensed Phase. *Chem. Rev.* **1995**, *95*, 1191–1201.
59. Lalevée, J.; Tehfe, M.-A.; Zein-Fakih, A.; Ball, B.; Telitel, S.; Morlet-Savary, F.; Graff, B.; Fouassier, J.P. *N*-Vinylcarbazole: An Additive for Free Radical Promoted Cationic Polymerization upon Visible Light. *ACS Macro Lett.* **2012**, *1*, 802–806.
60. Telitel, S.; Dumur, F.; Faury, T.; Graff, B.; Tehfe, M.-A.; Gigmès, D.; Fouassier, J.-P.; Lalevée, J. New core-pyrene  $\pi$  structure organophotocatalysts usable as highly efficient photoinitiators. *Beilstein J. Org. Chem.* **2013**, *9*, 877–890.
61. Lalevée, J.; Dumur, F.; Mayer, C.-R.; Gigmès, D.; Nasr, G.; Tehfe, M.-A.; Telitel, S.; Morlet-Savary, F.; Graff, B.; Fouassier, J.-P. Photopolymerization of *N*-Vinylcarbazole Using Visible-Light Harvesting Iridium Complexes as Photoinitiators. *Macromolecules* **2012**, *45*, 4134–4141.
62. Mokbel, H.; Dumur, F.; Telitel, S.; Vidal, L.; Xiao, P.; Versace, D.-L.; Tehfe, M.-A.; Morlet-Savary, F.; Graff, B.; Fouassier, J.-P.; *et al.* Photoinitiating systems of polymerization and *in situ* incorporation of metal nanoparticles into polymer matrices upon exposure to visible light: Push–pull malonate and malononitrile based dyes. *Polym. Chem.* **2013**, *4*, 5679–5687.
63. Lalevée, J.; Blanchard, N.; Graff, B.; Allonas, X.; Fouassier, J.P. Tris(trimethylsilyl)silyl *versus* tris(trimethylsilyl)germyl: Radical reactivity and oxidation ability. *J. Organomet. Chem.* **2008**, *693*, 3643–3649.
64. Zaborovskiy, A.B.; Lutsyk, D.S.; Prystansky, R.E.; Kopylets, V.I.; Timokhin, V.I.; Chatgililoglu, C. A mechanistic investigation of  $(\text{Me}_3\text{Si})_3\text{SiH}$  oxidation. *J. Organomet. Chem.* **2004**, *689*, 2912–2919.
65. Hua, Y.; Crivello, J.V. Synergistic interaction of epoxides and *N*-vinylcarbazole during photoinitiated cationic polymerization. *J. Polym. Sci. A: Polym. Chem.* **2000**, *38*, 3697–3709.
66. Abdoul-Rasoul, F.A.M.; Ledwith, A.; Yagci, Y. Photochemical and thermal cationic polymerizations promoted by free radical initiators. *Polymer* **1978**, *19*, 1219–1222.
67. Xiao, P.; Lalevée, J.; Zhao, J.; Stenzel, M.H. *N*-Vinylcarbazole as Versatile Photoinitiator of Photopolymerization under Household UV LED Bulb (392 nm). *Macromol. Rapid Commun.* **2015**, doi:10.1002/marc.201500214.
68. Scaiano, J.C.; Billone, P.; Gonzalez, C.M.; Maretta, L.; Marin, M.L.; McGilvray, K.L.; Yuan, N. Photochemical routes to silver and gold nanoparticles. *Pure Appl. Chem.* **2009**, *81*, 635–647.
69. McGilvray, K.L.; Decan, M.R.; Wang, D.; Scaiano, J.C. Facile Photochemical Synthesis of Unprotected Aqueous Gold Nanoparticles. *J. Am. Chem. Soc.* **2006**, *128*, 15980–15981.
70. Marin, M.L.; McGilvray, K.L.; Scaiano, J.C. Photochemical Strategies for the Synthesis of Gold Nanoparticles from Au(III) and Au(I) Using Photoinduced Free Radical Generation. *J. Am. Chem. Soc.* **2008**, *130*, 16572–16584.
71. Stampelcoskie, K.G.; Scaiano, J.C. Kinetics of the Formation of Silver Dimers: Early Stages in the Formation of Silver Nanoparticles. *J. Am. Chem. Soc.* **2011**, *133*, 3913–3920.
72. Sangermano, M.; Yagci, Y.; Rizza, G. *In Situ* Synthesis of Silver-Epoxy Nanocomposites by Photoinduced Electron Transfer and Cationic Polymerization Processes. *Macromolecules* **2007**, *40*, 8827–8829.

73. Yagci, Y.; Sangermano, M.; Rizza, G. A visible light photochemical route to silver-epoxy nanocomposites by simultaneous polymerization–reduction approach. *Polymer* **2008**, *49*, 5195–5198.
74. Yagci, Y.; Sangermano, M.; Rizza, G. *In situ* synthesis of gold-cross-linked poly(ethylene glycol) nanocomposites by photoinduced electron transfer and free radical polymerization processes *Chem. Commun.* **2008**, *24*, 2771–2773.
75. Nehlig, E.; Schneider, R.; Vidal, L.; Clavier, G.; Balan, L. Silver Nanoparticles Coated with Thioxanthone Derivative as Hybrid Photoinitiating Systems for Free Radical Polymerization. *Langmuir* **2012**, *28*, 17795–17802.
76. Buruiana, T.; Melinte, V.; Jitaru, F.; Buruiana, E.-C.; Balan, L. Preparation of siloxane-based urethane dimethacrylates carrying carboxylic groups and the effect of silver nanoparticles on the properties of composite polymer films. *Polym. Chem. Part A* **2012**, *50*, 874–883.

© 2015 by the authors; licensee MDPI, Basel, Switzerland. This article is an open access article distributed under the terms and conditions of the Creative Commons Attribution license (<http://creativecommons.org/licenses/by/4.0/>).